COMMUNICATION

ChemComm
www.rsc.org/chemcomm

Fabrication of Ni nanoparticles by selective oxidation of permalloy thin film during imidization of polyamic acid†

Sung K. Lim, Chong S. Yoon* and Chang K. Kim
Div. of Materials Engineering, Hanyang University, Seoul, Korea. E-mail: csyoon@hanyang.ac.kr; Fax: +82-2-2290-1838; Tel: +82-2-2290-0384

Received (in Cambridge, UK) 15th December 2003, Accepted 29th January 2004
First published as an Advance Article on the web 23rd February 2004

Ni nanoparticles embedded in a polyimide (PI) matrix were fabricated by selectively oxidizing a layer of $Ni_{80}Fe_{20}$ metal film sandwiched between two PI precursor layers. Ni nanoparticles, formed in a monolayer between two PI layers, had an average particle size of ~5 nm. X-Ray photoelectron spectroscopy confirmed that Fe in the film was preferentially consumed, resulting in the formation of Ni nanoparticles.

A magnetic nanoparticle array is increasingly envisioned as an alternative system for the next generation of magnetic data storage beyond 100 Gbit in^{-2}, which is thought to be unattainable using conventional continuous magnetic thin films.[1] Preparation of magnetic particles based on Co and FePt, however, often require organic additives to protect them from oxidation and aggregation.[2] It is also still questionable that such methods of producing nanoparticles can be scaled up to the required microscopic level. In this paper, we describe an economic method of fabricating metallic nanoparticles embedded in a polyimide (PI) matrix which provides the necessary magnetic isolation among particles.

Ni nanoparticles were fabricated by oxidizing a layer of $Ni_{80}Fe_{20}$ metal film sandwiched between two PI precursor. The PI precursor was prepared by spin coating the polyamic acid (PI2610D, Dupont) dissolved in *N*-Methyl-2-pyrrolidone (1 : 3 ratio by weight) on a Si wafer. The PI precursor thickness was adjusted such that the final cured PI was 40 nm thick. The PI precursor was subsequently treated at 135 °C for 30 min to evaporate the solvent. Using a DC magnetron sputterer, 3.5 nm thick $Ni_{80}Fe_{20}$ film was deposited onto the PI-coated substrate. After coating another layer of the PI precursor, the sample was held at room temperature for 24 hours. The PI/$Ni_{80}Fe_{20}$/PI stack was soft-baked at different temperatures and periods of time and then cured at 300–600 °C for 1 hour under vacuum (10^{-5} Torr). The fabrication process is illustrated in Fig. 1. Transmission electron microscopy (TEM, JEOL 2010) was used to characterize the synthesized nanoparticles. TEM samples were prepared by mechanical grinding and ion milling with a cold stage. For X-ray photoelectron spectroscopy (XPS, PH 5400), monochromatic X-ray generated from Al Kα (15 kV) was used.

It was previously shown that metal oxide nanoparticles nucleated in the PI matrix as a by-product of the imidization process when Fe, Cu and Sn thin films were inserted between two precursor layers.[3] However, when the $Ni_{80}Fe_{20}$ film is deposited, we observed a continuous layer of metallic film embedded in the PI matrix. When the initial thickness of the $Ni_{80}Fe_{20}$ film was decreased to 3.5 nm, the metal film broke up into ~5 nm sized particles. TEM images of the nanoparticles are shown in Fig. 2. The particles had a quite narrow size distribution with nearly spherical shapes. In fact, when the curing temperature was increased to 400 °C, the average particle size remained at 5 nm. The standard deviation of the particle size, however, decreased from 1.5 nm to 0.7 nm, thus tightening the size distribution. Further increase in curing temperature beyond 500 °C resulted in coarsening of the particles. The cross-sectional TEM micrograph in the inset of Fig. 2 (a) shows that these particles are arranged in a monolayer sandwiched between two PI layers. Because of the line broadening arising from the extremely small particle size, the electron diffraction pattern in Fig. 2 (b) could not be clearly indexed. The pattern, however, tentatively matched a fcc structure, which rules out that the particles are made from Fe.

Fig. 3 plots XPS spectra near the Fe and Ni 2p absorption edges from the cured sample. As can be seen from Fig. 2 (a), Fe $2p_{3/2}$ peak was shifted from its pure Fe peak (at 707 eV) to the high binding energy side by ~3 eV to nearly match the binding energy of Fe_2O_3. The measured Fe spectrum, in fact, closely resembled the pure γ-Fe_2O_3 spectrum with its symmetric peak profiles and characteristic satellite peaks.[4] Separation of the Fe spectrum clearly shows that a substantial amount of Fe from the $Ni_{80}Fe_{20}$ film was oxidized during imidization. In contrast, positions and shape of both Ni $2p_{3/2}$ and $2p_{1/2}$ peaks confirm that Ni mostly remained metallic. The XPS spectra suggest that Fe was selectively oxidized from the $Ni_{80}Fe_{20}$ film. Comparing the Gibbs free energies of two oxides indicates that Fe_2O_3 is more thermodynamically stable than NiO and that Fe is more likely to react with the carboxylic group on the polyamic

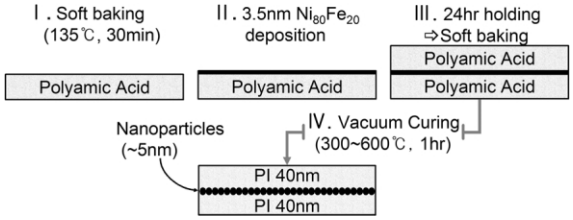

Fig. 1 Schematic illustration of the nanoparticle fabrication process.

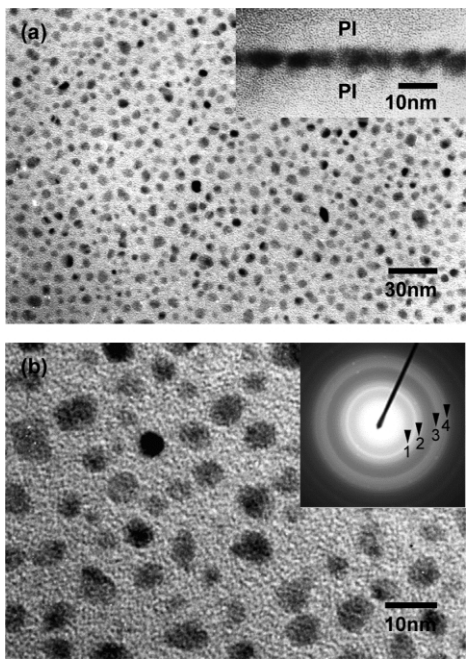

Fig. 2 (a) TEM image of the Ni nanoparticles produced by curing the PI/$Ni_{80}Fe_{20}$(3.5 nm)/PI stack at 300 °C. The inset shows the particles in a cross-sectional view, (b) enlarged image of (a). The inset shows the electron diffraction pattern obtained from the sample and is indexed as a fcc structure (1: (111), 2: (200), 3: (220), 4: (311)).

† Electronic supplementary information (ESI) available: histogram for the particle size distribution and FTIR spectra obtained at different curing temperatures. See http://www.rsc.org/suppdata/cc/b3/b316386e/

DOI: 10.1039/b316386e

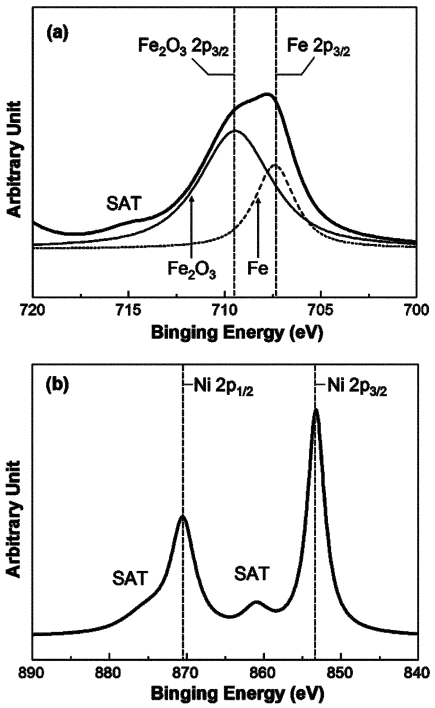

Fig. 3 XPS spectra from the PI/$Ni_{80}Fe_{20}$(3.5 nm)/PI sample cured at 300 °C: (a) Fe 2p with the peak-separated curves showing the contribution from Fe_2O_3 and Fe, (b) Ni 2p. Satellite peaks in (b) belong to metallic Ni while the peak in (a) belongs to γ-Fe_2O_3.

acid chain.[5] Judging from the XPS results, the fcc structure shown in Fig. 2 (b) resulted from the metallic Ni particles as Fe in the alloy film was preferentially consumed during imidization.

Fig. 4 shows the transmission FTIR spectra obtained from a PI film and the PI/$Ni_{80}Fe_{20}$(3.5 nm)/PI sample cured at 300 °C. Detailed analysis of the major peaks in the PI film can be found elsewhere.[6] Fig. 4 clearly shows that the structure of the PI film changed significantly when cured in the vicinity of the $Ni_{80}Fe_{20}$ film. The intensity loss of 1770, 1712 and 1621 cm^{-1} bands reflects the formation of Fe carboxylate group as the C=O carbonyl stretch is responsible for these bands. This result agrees well with the XPS data. Similar observations were also found when Cu, Cr and Co films were deposited on a cured PI film.[7] In addition to that, the bands ranging from 1600 cm^{-1} to 1400 cm^{-1}, corresponding to the aromatic ring vibration, also experienced a significant loss in intensity. This loss suggests that Fe also reacted with the aromatic rings, forming a metal complex during imidization. The 1360 cm^{-1} band from the C–N stretch remained unchanged, indicating that the chain structure of the PI was not destroyed. However, on increasing the curing temperature to 500 °C, all the bands were severely

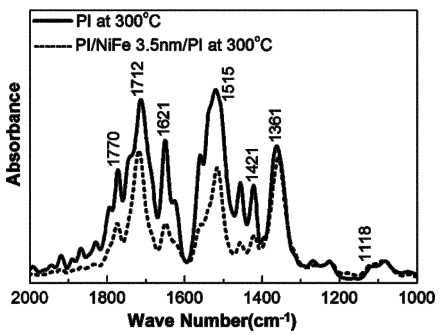

Fig. 4 FTIR spectra from the PI/$Ni_{80}Fe_{20}$(3.5 nm)/PI and PI with the metal film samples cured at 300 °C.

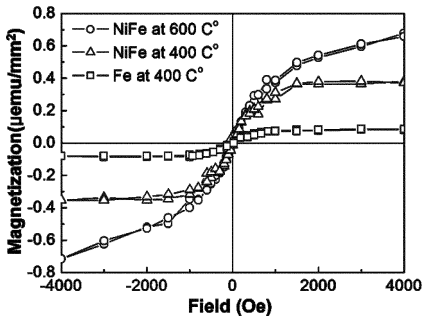

Fig. 5 Magnetic hysteresis loops from the PI/$Ni_{80}Fe_{20}$(3.5 nm)/PI and PI/Fe(3.5 nm)/PI samples cured at different temperatures.

reduced. The PI structure was effectively destroyed by the presence of a metallic film at this curing temperature. The FTIR result showed that there was an extensive reaction between metal and polyamic acid when the acid was cured in presence of the permalloy film. The XPS data indicated that this reaction was mainly confined to Fe so that Fe was preferentially consumed from the permalloy film.

In Fig. 5 are the magnetic hysteresis loops obtained from the PI/$Ni_{80}Fe_{20}$(3.5 nm)/PI samples cured at 400 °C and 600 °C as well as from the PI/Fe(3.5 nm)/PI sample. The loops were measured using a superconducting quantum interference device (SQUID) at room temperature. In general, the remanent magnetization for all samples was close to zero due to the superparamagnetic effect.[8] The saturation magnetization for the PI/$Ni_{80}Fe_{20}$(3.5 nm)/PI sample was, however, larger than that measured from the sample prepared from the pure Fe film because the pure Fe film oxidized to form ferrimagnetic γ-Fe_2O_3 particles, which are weakly magnetic. Since Ni has a much higher bulk magnetic moment than those of γ-Fe_2O_3 or antiferromagnetic NiO, Fig. 5 indicated the particles should be metallic Ni. As the curing temperature increased to 600 °C, the saturation magnetization rose due to the coalescence of nanoparticles and precipitation of Fe_2O_3 from metal complexes

In conclusion, we have demonstrated that by using a metal alloy film and sacrificing the more reactive metal, a monolayer of magnetic nanoparticles embedded in a non-magnetic medium can be fabricated. This method can be easily extended other alloy films to fabricate different metallic nanoparticles. It was also shown that the particle size and its distribution can be optimized by altering the imidization conditions.

This research was performed by the financial support of Center for Nanostructured Materials Technology under 21st Century Frontier R & D Programs of the Ministry of Science and Technology, Korea.

Notes and references

1 C. Haginoya, S. Heike, M. Ishibashi, K. Nakamura and K. Koike, *J. Appl. Phys.*, 1999, **85**, 8327.
2 J. W. Harrel, S. Wnag, D. E. Nikles and M. Chen, *Appl. Phys. Lett.*, 2001, **79**, 4393; C. Petit, A. Taleb and M. P. Pileni, *J. Phys. Chem B.*, 1999, **103**, 1805.
3 Y. Chung, H. P. Park, H. J. Jeon, C. S. Yoon, S. K. Lim, Y. H. Kim and Haginoya, *J. Vac. Sci. Technol. B.*, 2003, **21**(6), L9.
4 T. Fujii, F. M. F. de Groot, G. A. Sawatzky, F. C. Voogt, T. Hibma and K. Okada, *Phys. Rev. B*, 1999, **59**, 3195.
5 *The Oxide Handbook*, 2nd edn., ed. G. V. Samsonov, p. 45, IFI/Plenum, New York, 1982.
6 J. J. Pireaux, M. Vermeersch, C. Grégoire, P. A. Thiry and R. Caudano, *J.Chem. Phys.*, 1988, **88**, 3353.
7 Da-Yuan Shih, N. Klymko, R. Flitsch, J. Paraszczak and S. Nunes, *J. Vac. Sci. Technol. A*, 1991, **9**(6), 2963; D. S. Dunn and J. L. Grant, *J. Vac. Sci. Technol. A,*, 1989, **7**(2), 253.
8 D. Zanghi, C. M. Teodorescu, F. Petroff, H. Fischer, C. Bellouard, C. Clerc, C. Pélissier and A. Traverse, *J. Appl. Phys.*, 2001, **90**, 6367.